IUST International Journal of Engineering Science, Vol. **18,** *No.***3-4, 2007,** *Page* **39-45**
Industrial & Mechanical Engineering Special Issue

MESHLESS LOCAL PETROV-GALERKIN METHOD–STEADY, NON-ISOTHERMAL FLUID FLOW APPLICATIONS

A. Arefmanesh, M. Najafi, and H. Abdi

Abstract: *The meshless local Petrov-Galerkin method with unity as the weighting function has been applied to the solution of the Navier-Stokes and energy equations. The Navier-Stokes equations in terms of the stream function and vorticity formulation together with the energy equation are solved for a driven cavity flow for moderate Reynolds numbers using different point distributions. The L^2-norm of the error as a function of the size of the control volumes is presented for different cases; and the rate of convergence of the method is established. The results of this study show that the proposed method is applicable in solving a variety of non-isothermal fluid flow problems.*

Keywords: *meshless, control volume, Petrov-Galerkin, stream function, vorticity*

1. Introduction

Various meshless schemes have been introduced in recent years in order to circumvent the difficulties associated with mesh generation in the well-established numerical techniques, such as the finite element and the finite volume methods [1, 2]. Among the earliest so-called meshless techniques is "the diffuse element method" proposed by Nayroles et al. in which a collection of nodes and a boundary description are sufficient to obtain the Galerkin equations [3]. However, in this method, an auxiliary grid is still required to evaluate the integrals which result from applying the Galerkin method to the differential equations. Subsequently, via introducing a regular cell structure as the auxiliary grid, Belytschko et al. and Lu et al. transformed the above technique to the so-called element-free Galerkin method [4, 5].

In recent years, two other meshless technique – the meshless local boundary equation method, and the meshless local Petrov-Galerkin method (MLPG) – have been proposed by Zhu et al. and Atluri et al., respectively [6,7]. In these schemes, a local weak form of the differential equation over a local subdomain together with the shape function from moving least-squares interpolations are used to obtain the discretized equations. A recent comprehensive review of the MLPG method with emphasis on the solid mechanics applications can be found in Atluri's book [2].

Among other developments in the area of meshless techniques, one can mention the method of spheres proposed by De and Bathe [8] in which subdomains of spherical shapes are generated at every point in the domain. Subsequently, the dependant variables are interpolated within the spheres and the discretized equations are obtained by substituting the interpolations in the Galerkin weak form of the differential equation for the subdomains. Other truly meshless schemes that have been recently proposed and applied specifically to elasticity problems are the local point interpolation method by Gu and Liu [9], the regular hybrid boundary node method by Zhang et al. [10], and a modified meshless local Petrov-Galerkin method to elasticity problems in computer modeling and simulation by Hu et al. [11]. These schemes are based on the MLPG method with some degree of modifications.

There are also recent developments in the applications of meshless techniques to fluid flow and heat transfer problems. Arefmanesh et al. have applied a variation of the MLPG method with unity as the test function to the convection-diffusion, and potential flow equations [12]. The results show that the method combined with a proper upwinding scheme is very promising for obtaining accurate solutions to problems in the field of thermofluids. In a very recent paper Liu has used the MLPG approach based on discrete-ordinate equations to solve the radiative heat transfer problem in multi-dimensional absorbing-emitting-scattering semitrans-parent graded index media [13]. His results show that the MLPG method has a good accuracy in solving radiative heat transfer problems.

In this present study, the meshless local Petrov-Galerkin method with unity as the test function is applied to the solutions of the non-isothermal viscous flow equations. A variation of the streamline upwind Petrov-Galerkin (SUPG) technique based on adding optimal balancing diffusion along the streamlines is employed to obtain stable solution for high Peclet and Reynolds numbers. To establish the rate of convergence of the method, wherever possible, the L^2-norm of the error is also presented.

Paper first received Jun. 01, 2006 and in revised form Nov. 20, 2007.
A. Arefmanesh, Mech. Eng. Dept., Islamic Azad University, Science & Research Branch, a_aref32@yahoo.com
M. Najafi, Mech. Eng. Dept., Islamic Azad University, Science & Research Branch, m.njafi36@gmail.com
H. Abdi, Mech. Eng. Dept., Islamic Azad University, Science & Research Branch, h.abdi@seiau.ir

Due to the point distributions and control volume shapes flexibility of the method, the proposed meshless scheme suggests to be feasible in situations where fluid flow through reasonably complex narrow geometries exist.

2. Numerical Model

A bounded region Ω with the boundary $\Gamma = \Gamma_g \cup \Gamma_h$ in the two-dimensional space (Fig. 1) is considered. The steady incompressible fluid flow and energy equations written in terms of the stream function and vorticity in a dimensionless form are

$$\vec{\nabla}.\left(\vec{V}\omega\right) = \frac{1}{\mathrm{Re}}\nabla^2\omega \tag{1}$$

$$\nabla^2\psi = -\omega \tag{2}$$

$$\vec{\nabla}.\left(\vec{V}T\right) = \frac{1}{\mathrm{Pe}}\nabla^2 T \tag{3}$$

where, $\vec{V}$ is the dimensionless velocity vector with components $u = u^*/U$ and $v = v^*/U$ in the x and y directions, respectively, $\omega = \omega^* L/U$ is the dimensionless vorticity, $\mathrm{Re} = UL/\nu$ is the Reynolds number, $\mathrm{Pe} = UL/\alpha$ is the Peclet number, $\psi = \psi^*/UL$ is the dimensionless stream function, and $T = (T^* - T_{BW})/(T_{TW} - T_{BW})$ is the dimensionless temperature.

In the meshless local Petrov-Galerkin method with unity as the test function, hereafter named the meshless control volume method (MCVM) due to its similarity with the finite volume techniques, a collection of points is selected in the domain. Subsequently, a control volume is generated around each of the points. The control volumes have simple shapes such as circle or rectangle in the two-dimensional space. The size of the control volumes and the number of points belonging to each one of them can, in general, vary. Contrary to the usual control volume techniques, in this method the control volumes can intersect each other and overlap [14].

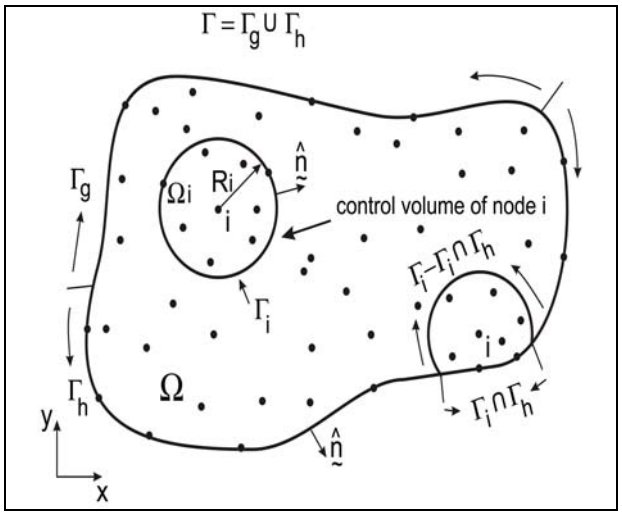

Fig 1. Domain Ω with two circular control volumes

As the next step in the numerical implementation of the MCVM, Eqs. (1), (2), and (3), are multiplied by the test function w. With w=1 the resulting expressions are then integrated over a typical control volume Ω_i. However, in order to obtain stable solutions for convection-dominated flows, a streamline upwind scheme is required [15, 16]. To apply the upwind technique to Eq. (1) as an example, this equation is first transformed to the streamline co-ordinates, s-t, with s pointing in the streamline direction and t being perpendicular to it. The resulting equation, after adding the artificial viscosity $1/\overline{\mathrm{Re}}$ properly, is

$$V\frac{\omega}{s} = \left(\frac{1}{\mathrm{Re}} + \frac{1}{\overline{\mathrm{Re}}}\right)\frac{\partial^2\omega}{s^2} + \frac{1}{\mathrm{Re}}\frac{\partial^2\omega}{t^2} \tag{4}$$

where, $V = (u^2 + v^2)^{1/2}$ is the magnitude of the velocity vector. The optimal artificial viscosity is obtained from [12, 16].

$$\frac{1}{\overline{\mathrm{Re}}} = \frac{V\bar{h}}{2}\left[coth\left(\frac{\mathrm{Re}^+}{2}\right) - \frac{2}{\mathrm{Re}^+}\right] \tag{5}$$

where, $\mathrm{Re}^+ = V\bar{h}/\nu$ is the local Reynolds number. The magnitude of $\bar{h}$ for uniform point distribution cases, is $\bar{h} = 2h(|u| + |v|)/V$ with h being the distance between two consecutive points. Transforming Eq. (4) back to the x-y co-ordinates yields

$$u\frac{\partial\omega}{\partial x} + v\frac{\partial\omega}{\partial y} = \frac{1}{\mathrm{Re}}\left(\frac{\partial^2\omega}{\partial x^2} + \frac{\partial^2\omega}{\partial y^2}\right) + V\frac{\omega}{s} = \left(\frac{1}{\mathrm{Re}} + \frac{1}{\overline{\mathrm{Re}}}\right)\frac{\partial^2\omega}{s^2} + \frac{1}{\mathrm{Re}}\frac{\partial^2\omega}{t^2} \tag{6}$$

Following a similar procedure as above, the energy equation for convection-dominated cases can be written as

$$u\frac{\partial T}{\partial x} + v\frac{\partial T}{\partial y} = \frac{1}{\mathrm{Pe}}\left(\frac{\partial^2 T}{\partial x^2} + \frac{\partial^2 T}{\partial y^2}\right) + \frac{1}{\overline{\mathrm{Re}}} = \frac{V\bar{h}}{2}\left[coth\left(\frac{\mathrm{Re}^+}{2}\right) - \frac{2}{\mathrm{Re}^+}\right] \tag{7}$$

The optimal artificial diffusivity used in the above equation is obtained from

$$\frac{1}{\overline{\mathrm{Pe}}} = \frac{V\bar{h}}{2}\left[coth\left(\frac{Pe^+}{2}\right) - \frac{2}{\mathrm{Pe}^+}\right] \tag{8}$$

where, $\mathrm{Pe}^+ = V\bar{h}/\alpha$.

Multiplying Eqs. (2), (6), and (7) by the test function w=1, and integrating the resulting equations over Ω_i

give, after integration by parts, the following weak forms of the vorticity, stream function, and energy equations, respectively for a typical control volume.

$$\int_{\Gamma_i} \vec{V}\omega.\hat{n}d\Gamma = \frac{1}{\mathrm{Re}}\int_{\Gamma_i}\frac{\omega}{n}d\Gamma + \frac{1}{\mathrm{Re}}\int_{\Gamma_i}\left(u\frac{\partial\omega}{\partial x}+v\frac{\partial\omega}{\partial y}\right)\frac{\vec{V}}{V^2}.\hat{n}d\Gamma \quad (9)$$

$$\int_{\Gamma_i}\frac{\psi}{n}d\Gamma = -\int_{\Omega_i}\omega d\Omega \quad (10)$$

$$\int_{\Gamma_i}\vec{V}T.\hat{n}d\Gamma = \frac{1}{\mathrm{Pe}}\int_{\Gamma_i}\frac{\partial T}{\partial n}d\Gamma + \frac{1}{\mathrm{Pe}}\int_{\Gamma_i}\left(u\frac{\partial T}{\partial x}+v\frac{\partial T}{\partial y}\right)\frac{\vec{V}}{V^2}.\hat{n}d\Gamma \quad (11)$$

where, Γ_i is the boundary of the Ω_i, $\hat{n}$ is the unit outward normal to the Γ_i. After solving for the stream function and vorticity, pressure can be obtained from the following Poisson equation [17]

$$\nabla^2 P = 2\left[\frac{\partial^2\psi}{\partial x^2}\frac{\partial^2\psi}{\partial y^2}-\left(\frac{\partial^2\psi}{\partial x\partial y}\right)^2\right]. \quad (12)$$

Multiplying Eq. (12) by unity weight function, and integrating the resulting equation by parts yield the following weak form of pressure equation for a typical control volume

$$\int_{\Gamma_i}\frac{\partial P}{\partial n}d\Gamma = \int_{\Omega_i} 2\left[\frac{\partial^2\psi}{\partial x^2}\frac{\partial^2\psi}{\partial y^2}-\left(\frac{\partial^2\psi}{\partial x\,\partial y}\right)^2\right]d\Omega \quad (13)$$

where, the right hand-side can be calculated after solving for the stream function.

To obtain the discretized equation of the control volume Ω_i, which contains n points, the unknown field, e.g. the vorticity, is approximated within Ω_i by [18]

$$\omega(x,y)\cong\overline{\omega}^{(i)}(x,y)=\sum_{l=1}^{m}P_l(x,y)\alpha_l=\mathbf{P}^T(x,y)\boldsymbol{\alpha} \quad (14)$$

where, $\boldsymbol{\alpha}=[\alpha_1,\alpha_2,...,\alpha_m]^T$ and the elements of the vector $\mathbf{P}(x,y)$, $P_l(x,y)$, $l=1(1)m$, are, in general, monomials. Approximations similar to Eq. (14) are also used for the unknown stream function and temperature fields.

Setting the approximation, Eq. (14), equal to the value of the $\omega(x,y)$ at the n points belonging to the control volume yields

$$\boldsymbol{\omega}=\begin{Bmatrix}\omega_1\\ \vdots\\ \omega_n\end{Bmatrix}=\begin{Bmatrix}\boldsymbol{P}_1^T\\ \vdots\\ \boldsymbol{P}_n^T\end{Bmatrix}\boldsymbol{\alpha}=\boldsymbol{C}\boldsymbol{\alpha} \quad (15)$$

where, $\omega_j=\omega(x_j,y_j)$ is the magnitude of the ω at the point (x_j,y_j), and $\mathbf{P}^T{}_j=\mathbf{P}^T(x_j,y_j)$ is the transpose of vector of monomials at this point. The elements of matrix C are $C_{jl}=p_l(x_j,y_j)$, $l=1(1)m$, $j=1(1)n$. If the number of points belonging to the control volume n is equal to the number of monomials of the vector $\mathbf{P}(x,y)$, m, the performed interpolation will be exact at the points (i.e., it will be equal to the value of the unknown function at the points), and the vector $\boldsymbol{\alpha}$ will be given by

$$\boldsymbol{\omega}=\begin{Bmatrix}\omega_1\\ \vdots\\ \omega_n\end{Bmatrix}=\begin{Bmatrix}\mathbf{P}_1^T\\ \vdots\\ \mathbf{P}_n^T\end{Bmatrix}\boldsymbol{\alpha}=\mathbf{C}\boldsymbol{\alpha} \quad (16)$$

the approximation $\overline{\omega}^{(i)}(x,y)$, in this case, is expressed by

$$\overline{\omega}^{(i)}(x,y)=\sum_{j=1}^{n}\phi_j^{(i)}(x,y)\omega_j \quad (17)$$

where, $\phi_j^{(i)}(x,y)$ with j=1(1)n, are the usual interpolation function (i.e., Lagrange polynomials) and ω_j with j=1(1)n, are the nodal values of the unknown function at the points.

The interpolation functions, which satisfy the standard conditions $\phi_j^{(i)}(x_l,y_l)=\delta_{jl}$ (δ_{jl} being the Kronocker delta) are given by [16, 17]

$$\phi_j^{(i)}(x,y)=\sum_{l=1}^{m}P_l(x,y)C_{lj}^{-1}, \quad j=1(1)n. \quad (18)$$

The control volumes which are employed in this study are rectangular and contain nine points each, n=9. The vector $\mathbf{P}(x,y)$, which is used in this case, has nine elements, m=9, and its transpose is $\boldsymbol{P}^T{}_{(x,y)}=[1,x,y,xy,x^2,y^2,x^2y,xy^2,x^2y^2]$.

Substituting this vector of monomials into Eq. (18) yields the biquadratic interpolation functions to be used for all the test cases in this study.

If the number of points belonging to the control volume is greater than the number of monomials of the vector $\mathbf{P}(x,y)$ (i.e., $n>m$), the approximation will still be given by (17); however, the interpolation functions are now written as follows [18]:

$$\omega = \begin{Bmatrix} \omega_1 \\ M \\ \omega_n \end{Bmatrix} = \begin{Bmatrix} P_1^T \\ M \\ P_n^T \end{Bmatrix} \alpha = C\alpha \qquad (19)$$

where, $\boldsymbol{D}^{-1} = \boldsymbol{A}^{-1}\boldsymbol{B}$, $\boldsymbol{A} = \sum_{j=1}^{m} \boldsymbol{P}(x_j, y_j)\boldsymbol{P}^T(x_j, y_j)$, and $\boldsymbol{B} = \left[\boldsymbol{P}(x_1, y_1), \boldsymbol{P}(x_2, y_2), ..., \boldsymbol{P}(x_n, y_n)\right]$.

Substituting the approximation $\overline{\omega}^{(i)}(x, y)$ and similar approximations for the stream function and temperature into Eqs. (9), (10), and (11), yield the discretized equations for Ω_i. Using the same procedure for every control volume gives the system of the discretized equations for all the points within the domain.

Solving the system of algebraic equations yields the unknown variables at the points. Having obtained the stream function, the right hand-side of Eq. (13) is calculated.

To acquire the pressure distribution, its interpolation within a control volume is substituted into Eq. (13) yielding the discretized equation. The pressure distribution is obtained after solving the system of discretized equations for pressure for all the control volumes.

Due to the existence of the convective terms within the energy as well as the vorticity equations, the obtained stiffness matrices are asymmetric. However, the global stiffness matrix for the stream function equation (the Poisson equation) is symmetric. Moreover, the resulting global matrices for the MCVM method are diagonally dominant.

Additionally, due to the coupling of the vorticity equation with the stream function equation, the resulting stiffness matrices are non-linear; hence, an iterative scheme is utilized to obtain the solutions. Because of the non-linearity, and the coupling, the condition numbers during the iteration scheme are constantly varying. However, for a linear matrix such as that obtained in a pure heat conduction problem, the condition number using this proposed method is a constant. For a pure conduction in a square domain using the MCVM method with a regular 11×11 uniform point distribution [12], the condition number based on infinity norm is equal to 39.6. The condition number for the same problem using the standard finite volume method with the same control volume size is equal to 58.5.

For other point distributions and mesh sizes, the condition numbers of the two schemes are comparable. The following examples demonstrate the method implementation.

3. Results

Equations (9), (10), and (11) are solved for the lid-driven cavity flow as a test case. The domain, the boundary conditions, the point distribution, and a typical control volume for the driven cavity flow are shown in Fig. 2. The control volume contains nine points. The shape functions are biquadratic [16] and the interpolation is exact in this case. A 33×33 nonuniform point distribution is employed for the numerical simulations.

The streamlines for the driven cavity flow for $\mathrm{Re}=100$ are shown in Fig. 3. Figure 4 shows a comparison of the cavity horizontal centerline velocity for $\mathrm{Re}=100$, obtained by the MCVM, with the results of the finite element method, FEM [19].

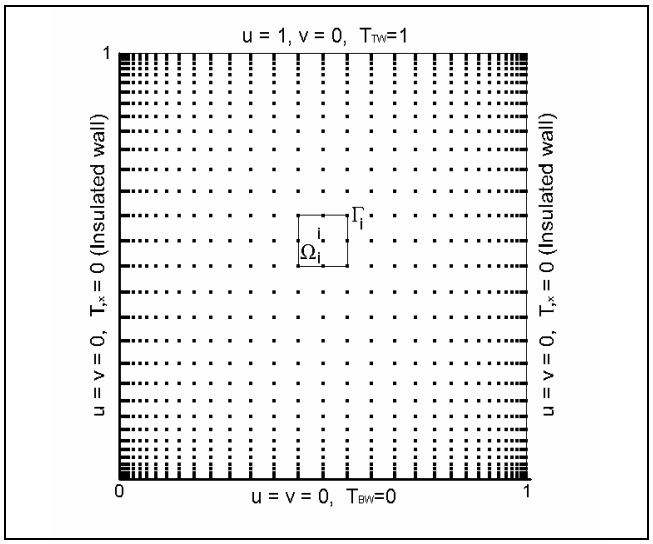

Fig 2. A 33×33 no uniform point distribution for lid-driven cavity flow

Various no uniform point distributions with increasing degree of refinement have been employed for the MCVM results in this figure.

Convergence of the MCVM results to a unique velocity is demonstrated in this figure. The converged velocity is in good agreement with the results of the finite element method.

Fig. 5 shows the discrete L^2-norms of the error for the stream function and vorticity for $\mathrm{Re}=100$ and 400. The convergence of the MCVM results with decreasing the size of the control volumes is demonstrated in this figure. The rate of convergence, as observed from the figure, is nearly quadratic. The isotherms for the driven cavity flow for $\mathrm{Pe}=50$, $\mathrm{Re}=100$, and the thermal boundary conditions shown in Fig. 2, are depicted in Fig. 6.

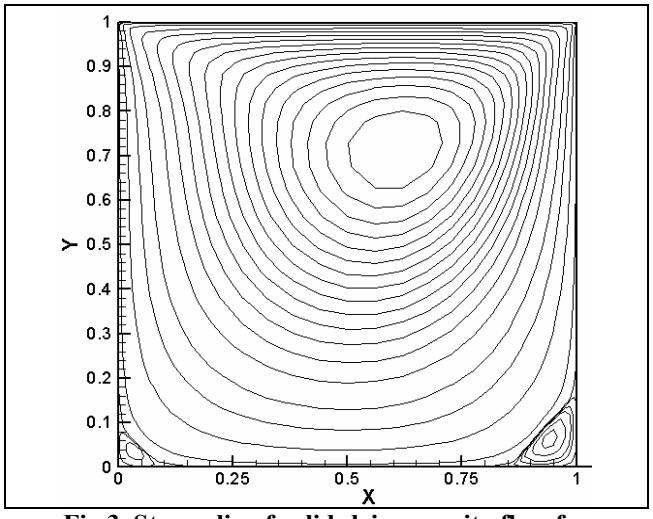

Fig 3. Streamline for lid-driven cavity flow for Re=100

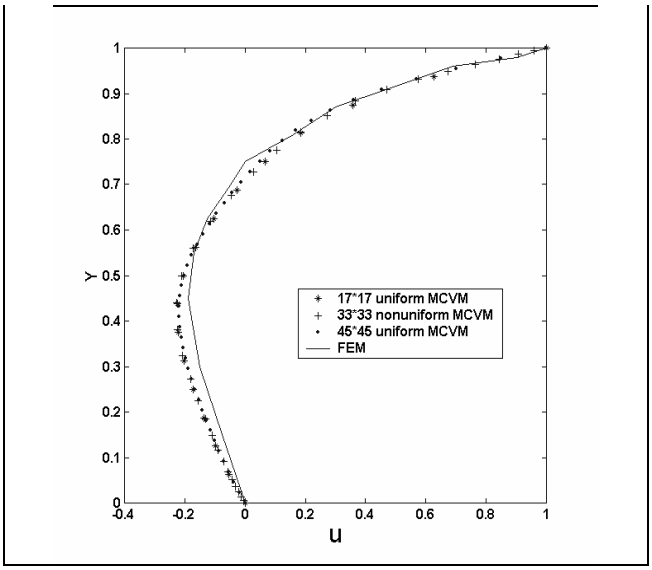

Fig 4. Cavity horizontal centerline velocities for Re=100, comparison of MCVM with FEM results[19]

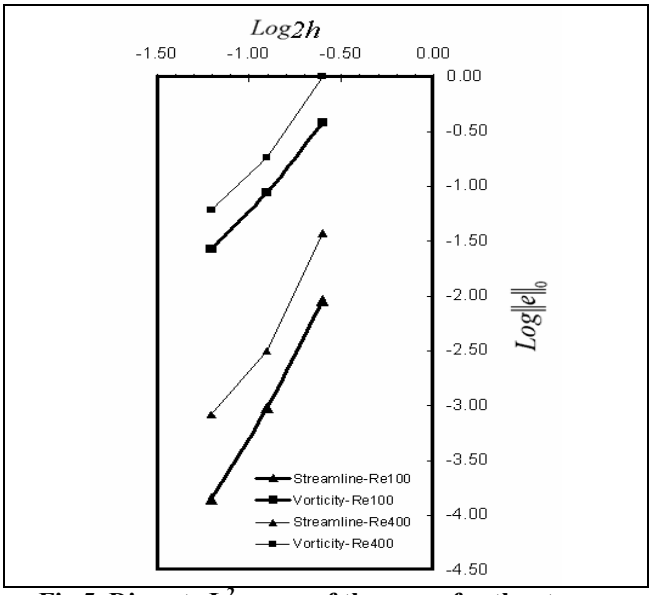

Fig 5. Discrete L^2-norm of the error for the stream function and vorticity for Re=100 and 400

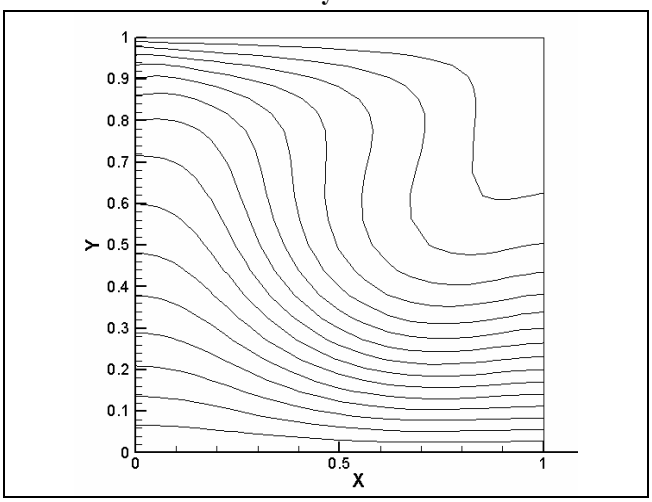

Fig 6. Isotherms of the lid-driven cavity flow for Re=100 and Pe=50

Figs. 7 and 8 show the streamline and the horizontal centerline velocity for the driven cavity flow for Re =400, respectively. In Fig. 8 the horizontal centerline velocity obtained by the MCVM using different point distributions are compared with those obtained by the finite difference method (FDM) employing a pure stream-function formulation [20]. The convergence of the MCVM results to the results of the finite difference method with decreasing the size of the control volumes is clearly observed in this figure.

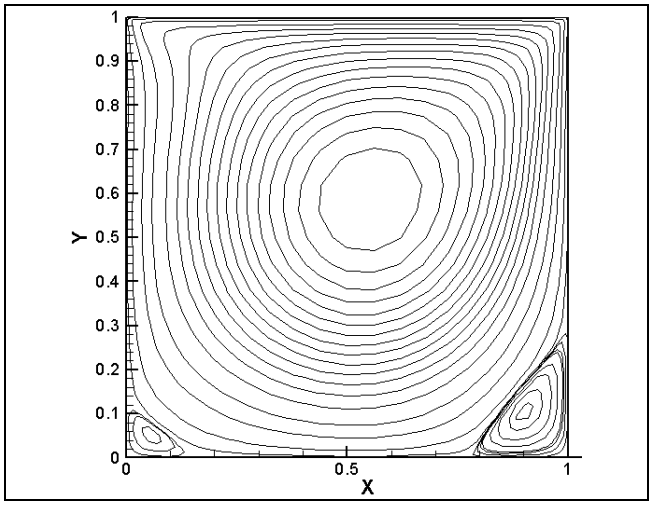

Fig7. Streamlines for the lid-driven cavity flow for Re=400

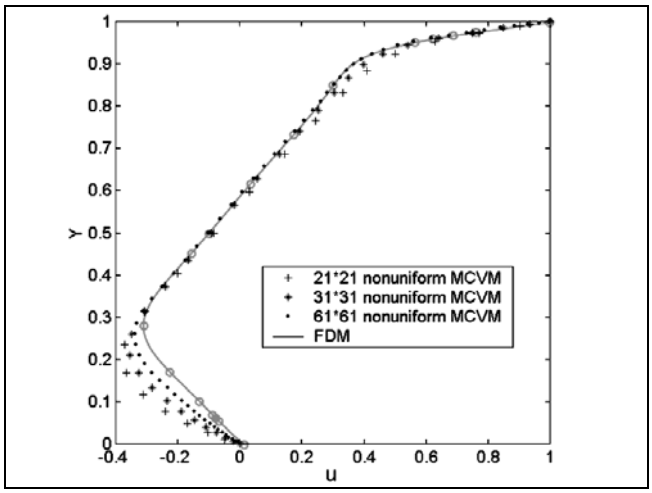

Fig 8. Cavity horizontal centerline velocity for Re=400, comparisons of MCVM with FDM results [20]

4. Conclusions

A meshless local Petrov-Galerkin method with the weighting function of unity is applied to the solution of the Navier-Stokes as well as energy equations for a lid-driven cavity flow test case. Reynolds numbers of 100 and 400 were considered for the driven cavity flow with non-uniform point distributions for the implemented numerical method. The streamlines as well as the cavity horizontal centerline velocities obtained through the proposed method were compared with those of the finite element, and the finite difference methods implemented by other investigators. The comparisons show very close

agreement, and even coincidence for some substantial portions of the domain.

The discrete L^2-norms of the error for the stream function and the vorticity show nearly quadratic convergence rate.

Based on the obtained results and their comparisons with other numerical methods, the accuracy of the proposed method is established, hence the method proves to be applicable for solving non-isothermal fluid flow problems.

References

[1] Atluri, S.N., & Shen, S., "*The meshless local Petrov-Galerkin (MLPG) method",* Tech. Science Press, USA, 2002.

[2] Atluri, S.N., *"The meshless method (MLPG) for domain and bie discretization*", Tech. Science Press, USA, 2004.

[3] Nayrols, B., Touzot, G., & Villon, P., *"Generalizing the FEM: diffuse approximation and diffuse elements,"* Comput. Mech., 10, 1992, PP. 307-318.

[4] Belytschko, T., Krongauz, Y., Organ, D., Flemming, M., & Krysl, P., *"Meshless methods: An overview and recent developments*," Comput. Methods Appl. Mech. Eng., 139, 1996, PP. 3-47.

[5] Lu, Y.Y., Belytschko, T., & Gu, L., *"A new implementation of the element-free galerkin method*," Comput. Methods Appl. Mech. Eng., 113, 1994, PP. 397-414.

[6] Zhu, T., Zhang, T.D., & Atluri, S.N., *"A meshless local boundary integral equation (LBIE) method for solving nonlinear problems,*" Comput. Mech., 22, 1998, PP. 174-186.

[7] Atluri, S.N., & Zhu, T., *"The local Petrov-Galerkin (MLPG) approach for solving problems in Elasto-Statics,"* Comput. Mech., 25, 2000, PP. 169-179.

[8] De, S., & Bathe, K.J., *"The method of finite spheres with improved numerical integration,"* Comput. & Truct., 79, 2001, PP. 2183-2196.

[9] Gu, Y.T., & Liu, G.R., *"A local point interpolation method for static and dynamic analysis of thin beams,*" Comput. Methods Appl. Mech. Eng., 190, 2001, PP. 5515-5528.

[10] Zhang, J., & Yao, Z., *"The regular hybrid boundary node method for three-dimensional linear elasticity,"* Eng. Analysis Boundary Elem., 28, 2004, PP. 525-534.

[11] Hu, DA., Long, S.Y., Liu, K.Y., & Li, G.Y., *"A modified meshless local Petrov-Galerkin method to elasticity problems in computer modeling and simulation,*" Eng. Analysis Boundary Elem., 30, 5, 2006, PP. 399-404.

[12] Arefmanesh, A., Najafi, M., & Abdi, H., *"A meshless local Petrov-Galerkin method for fluid dynamics and heat transfer applications,"* J. of Fluids Eng., 127, 2005, PP. 647-655.

[13] Liu, L.H., "*Meshless method for radiation heat transfer in graded index medium*," Int. J. Heat Mass Transfer, 49, 2006, PP. 219-229.

[14] Versteeg, H.K., & Malalasekera, W., *"An introduction to computational fluid dynamics, The finite volume method*", Longman, Loughborough, England, 1995.

[15] Brooks, A.N., & Hughes, T.J.R., "*Streamline upwind/ Petrov-Galerkin formulation for convection dominated flows with particular emphasis on the incompressible Navier-Stoks equations,*" Comp. Methods Appl. Mech. Eng., 32, 1982, PP. 199-258.

[16] Heinrich, J.C., & Pepper, D.W., "*Intermediate finite element method"*, Taylor and Francis, USA, 1999.

[17] Hoffmann, K.A., & Chiang, S.T., *"Computational fluid dynamics for engineers*," Engineering Education System, 1993.

[18] Oñate, E., Indelsohn, S., Zienkiewicz, O.C., & Taylor, R., "*A finite point method in computational mechanics: Applications to convective transport and fluid flow,*" Int. J. Numer. Methods Eng., 39, 1996, PP. 3839-3866.

[19] Reddy, J.N., & Gartling, D.K., *"The finite element method in heat transfer and fluid dynamics*", CRC Press, 2001.

[20] Kupferman, R., *"A central-difference scheme for a pure stream function formulation of incompressible viscous flow,"* SIAM J. Sci. Comput., Vol. 23, No. 1, 2001, PP. 1-18.

Nomenclature

h	:	distance between two consecutive points
L	:	domain length
N	:	total number of points
P	:	pressure
Pe	:	Peclet number
q	:	heat flux
R	:	radius
Re	:	Reynolds number
T	:	temperature
U	:	lid velocity
V	:	velocity
W	:	weighting function

Greek Symbols

α	:	thermal diffusivity
ϕ	:	interpolation function
Γ	:	boundary
Γ_g,Γ_h	:	boundary segments
ν	:	kinematic viscosity
ρ	:	density
Ω	:	domain

ω : vorticity
ψ : stream function

Subscripts
i: point or control volume number
BW: bottom wall
TW: top wall

Superscripts
*: physical variable
−: dimensionless variable, balancing coefficient
∧: unit vector
+: local variable
→: vector